ELSEVIER

Organic Electronics 1 (2000) 33–40

Organic Electronics

www.elsevier.nl/locate/orgel

Color characterization of large area polymer image sensors

J. Wang [a,b], G. Yu [a], G. Srdanov [a], A.J. Heeger [a,b,*]

[a] *UNIAX Corporation, 6780 Cortona Drive, Santa Barbara, CA 93117-3022, USA*

[b] *Institute for Polymers and Organic Solids, University of California at Santa Barbara, Santa Barbara, CA 93106-5090, USA*

Received 18 May 2000; accepted 12 July 2000

Abstract

Large area image sensors made with semiconducting polymers are demonstrated to have true-color resolution (24-bits). The red, green and blue color primaries are achieved by coupling a set of color filters with the polymer sensor; the color-sensing pixels are fabricated from a single polymer with photoresponse that covers the visible spectral range from 400 to 700 nm. A process for recovering the image from the pixelated photocurrent data is developed; the image recovery process is general and applicable to image arrays with power-law light intensity dependence and with finite pixel dark current. Large size, true-color images were processed by scanning with a linear array of polymer photodiodes.

1. Introduction

Optoelectronic phenomena in semiconducting (conjugated) polymers have attracted broad attention in recent years [1–3]. Since the discovery of electroluminescence (EL) from poly(*p*-phenylene vinylene) [4] and its soluble derivatives [5], research has focused on developing an understanding of the device physics [6] and on improvement of the device performance to levels suitable for practical applications. Passively *x–y* addressable polymer emissive displays have been demonstrated with luminous efficiencies of 3–5 lm/Watt and operating lifetimes of more than 10^4 h [1,2,7–9]. Moreover, significantly improvement of EL efficiencies can be anticipated [10].

In the polymer light emitting diode, electrons and holes are injected into the semiconducting polymer film at the cathode and anode, respectively. The electrons and holes subsequently recombine radiatively within the polymer, and photons are emitted. The inverse process, photogeneration of electric current, offers promise for large area photovoltaic and photosensing applications [1,2]. High efficiency polymer photovoltaic cells, photodiodes and optocouplers have been demonstrated [11–14]. More recently, large area, true-color, digital image sensors have been successfully demonstrated using photodiode arrays made with semiconducting polymers [15]. These polymer image sensors show high photosensitivity, low dark current, large dynamic range and 24-bit color resolution.

For image sensing applications in the visible spectral range, the sensing material must absorb light with wavelengths between 400 and 700 nm. To achieve high quality digital images, the dynamic range of the photosensor must be larger than 256 (to enable images with at least 8-bit gray levels). For image sensors with color recognition, the image

* Corresponding author. Tel.: +1-805-8933184, +1-305-893-2001; fax: +1-805-8934755.

E-mail address: ajh@physics.ucsb.edu (A.J. Heeger).

1566-1199/00/$ - see front matter
PII: S1566-1199(00)00006-9

pixels must separate the color information into three primary colors (such as red, green and blue, or their complementary colors cyan, magenta and yellow). This color information must then be correctly interpreted in the process of reproduction of color images. In this article, we study the color separation and reproduction processes with a large area polymer image sensor. Color images were achieved by coupling wide-band polymer photodiodes with color filters. The working primaries are used to make color images that faithfully reproduce the original picture. High quality color reproduction is demonstrated by matching the overall spectral response of the sensing system to the color-response of human vision.

2. Device fabrication

There are two common approaches in the construction of red, green and blue color pixels for image sensors. The first is to combine three monocolor pixels made with different sensing materials that exhibit spectral response to three primary colors within the spectral range. The second is to use three photosensors made with a single sensing material with a photoresponse spectrum that covers the entire visible range. In the latter case, color recognition is achieved by combining the three wide-band pixels with a set of color filters. Although both approaches have been adopted in the display industry, the first approach offers the advantage of higher device efficiency. The second approach has been the favorite for image sensors because the fabrication process is relatively easy and because of the relative simplicity of achieving saturated colors.

The color filter approach (with a single sensing material) was chosen to construct the color pixels of the polymer image sensors used for this study. Regioregular poly(3-hexyl thiophene), P3HT, a semiconducting polymer with an optical gap of $\sim$1.8 eV (670 nm), was utilized as the sensing material. The photosensitivity of P3HT can be enhanced significantly by blending with a photosensitizer such as C_{60} or soluble fullerene derivatives such as 1-(3-methoxycarbonyl)propyl-1-phenyl-[6,6]C_{61}, [6,6]PCBM. The enhanced photosensitivity of the blend over that of the pure semiconducting polymer results from ultrafast photoinduced electron transfer from P3HT to the fullerene acceptor [16,17]. The onset of the photoresponse of the P3HT:PCBM blend is nearly the same as that of P3HT, with a small tail extending beyond 700 nm as a result of absorption by the PCBM. The molecular structures of these components are shown in Fig. 1. Fig. 2 shows the spectral response of a photodiode made using indium/tin-oxide (ITO) as the anode and aluminum (Al) as the cathode in the ITO/P3HT:PCBM/Al thin film (sandwich) structure.

A linear photodiode array was made as shown in Fig. 3, with each pixel in the ITO/P3HT:PCBM/Al diode configuration. The ITO layer was patterned by photolithography into 102 strips, each 450 μm in width. The space between adjacent ITO strips was 185 μm. The pitch size was thus 635 μm. The P3HT:PCBM blend solution was prepared by mixing master solutions of P3HT and PCBM with 1:1 weight ratio. The blend film was spin-cast from the solution onto the ITO/glass substrate at room temperature; the polymer film was not patterned. A strip of aluminum (635 μm wide) was thermally evaporated onto the surface of P3HT:PCBM film and served as the common cathode of the linear array. The whole length of the photodiode array was 2.55 inch with 40 dpi resolution in both directions.

A unique feature of this image array is that the sensing area of each pixel is defined by the patterned electrodes [15]. No patterning of the photoactive polymer layer is involved. This feature simplified the fabrication process and the corresponding cost considerably. The processability of the photosensing materials also allows such sensor arrays being fabricated in desired shapes for nonplanar image sensing. By using flexible substrate materials, flexible polymer photodiode arrays were demonstrated in UNIAX recently [18].

3. Theory of color sensing

Color recognition is based on the theory that any color can be decomposed into three primary colors [19],

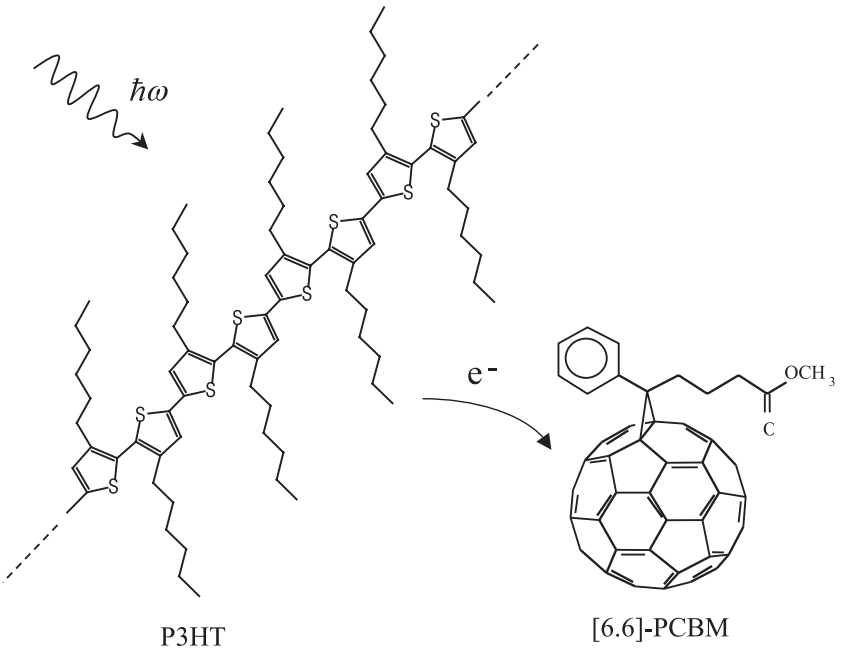

Fig. 1. Molecular structures of head-to-head regioregular P3HT and [6,6]PCBM.

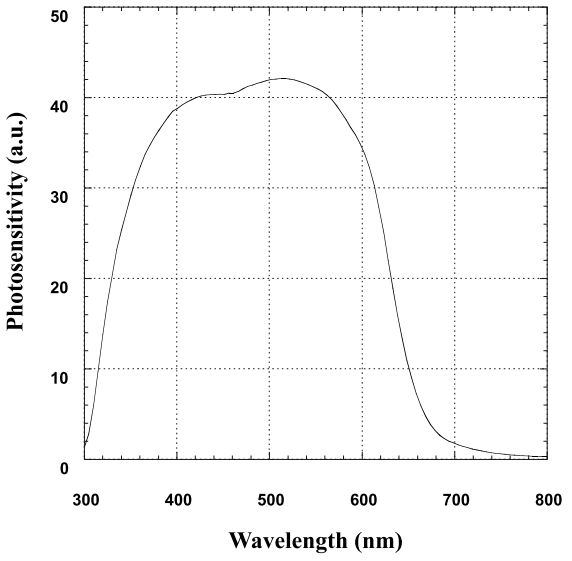

Fig. 2. Spectral response of a photodiode sensing pixel with the ITO/P3HT:PCBM/Al structure.

$$C = A_R R + A_G G + A_B B, \tag{1}$$

where C represents any color, and A_R, A_G and A_B are the relative amounts of each primary color R, G and B. In the human visual system, the A_R, A_G and A_B values are determined by integrating the human vision color-matching functions over the visible spectrum [20,21],

$$A_R = \int \beta(\lambda) S(\lambda) \bar{r}(\lambda)\, d\lambda, \tag{2a}$$

$$A_G = \int \beta(\lambda) S(\lambda) \bar{g}(\lambda)\, d\lambda, \tag{2b}$$

$$A_B = \int \beta(\lambda) S(\lambda) \bar{b}(\lambda)\, d\lambda, \tag{2c}$$

where $\beta(\lambda)$ is the spectral reflectance/transmittance of the object, $S(\lambda)$ is the spectral power distribution of the illumination, and $\bar{r}(\lambda)$, $\bar{g}(\lambda)$, $\bar{b}(\lambda)$ are the human visual color-matching functions defined with respect to chosen primaries.

The CIE 1931 standard color-matching functions are shown in Fig. 4. Since $\bar{r}(\lambda)$, $\bar{g}(\lambda)$, $\bar{b}(\lambda)$ have negative as well as positive values, the R, G, B amounts can be negative. This fact leads to the conclusion that additive color reproduction systems, such as displays, scanners, etc. cannot produce

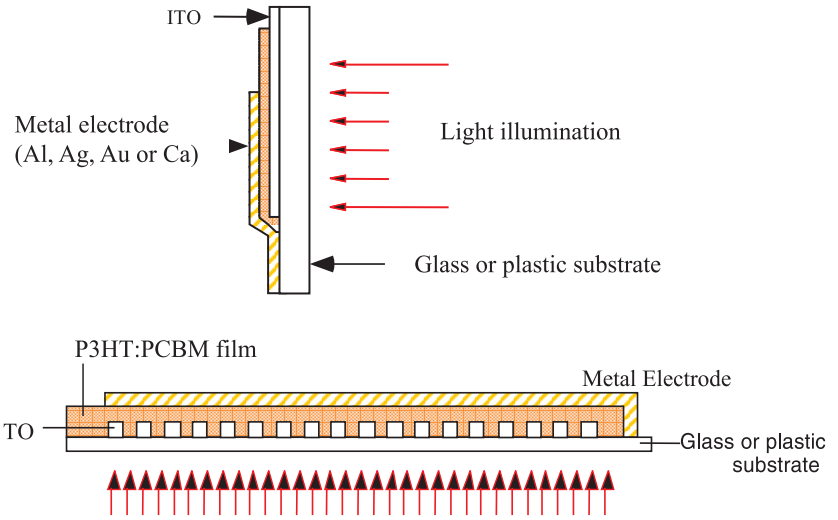

Fig. 3. Cross-section views of the polymer photodiode and the photodiode arrays.

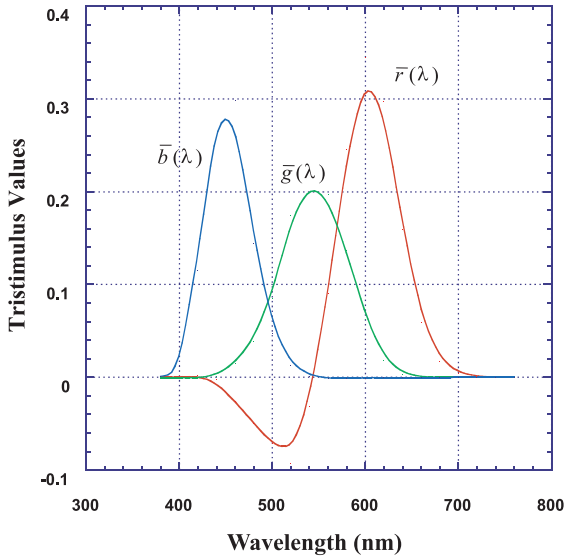

Fig. 4. Color-matching functions for the CIE 1931 Standard Colorimetric Observer with respect to the primaries Red at 700 nm, Green at 546.1 nm and Blue at 435.8 nm.

all the colors that can be detected by the human eye.

In color sensing systems, the amounts of each primary color are determined by the following [22]:

$$A_{\mathrm{R}}^{\mathrm{S}} = \int \beta(\lambda) S^{\mathrm{S}}(\lambda) F_r(\lambda) P(\lambda)\,\mathrm{d}\lambda, \tag{3a}$$

$$A_{\mathrm{G}}^{\mathrm{S}} = \int \beta(\lambda) S^{\mathrm{S}}(\lambda) F_g(\lambda) P(\lambda)\,\mathrm{d}\lambda, \tag{3b}$$

$$A_{\mathrm{B}}^{\mathrm{S}} = \int \beta(\lambda) S^{\mathrm{S}}(\lambda) F_b(\lambda) P(\lambda)\,\mathrm{d}\lambda. \tag{3c}$$

In Eqs. (3a)–(3c), the superscript S denotes the scanning system, $P(\lambda)$ is the spectral response of the sensor, and $F_r(\lambda)$, $F_g(\lambda)$ and $F_b(\lambda)$ are

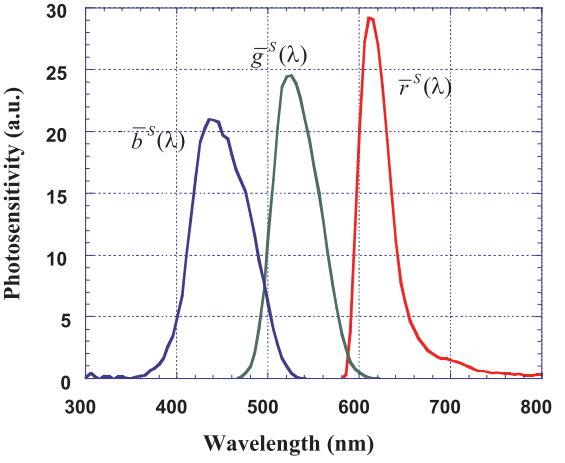

Fig. 5. The color-matching functions of our sensing systems with filters.

the spectral transmittances of the color filters. The color-matching functions $\bar{r}^S(\lambda)$, $\bar{g}^S(\lambda)$, $\bar{b}^S(\lambda)$ of the sensing system can be defined as $F_{r,g,b}(\lambda)P(\lambda)$.

The color-matching functions of the color pixels were determined by measuring the spectral responses of the ITO/P3HT:PCBM/Al photodiodes with red, green and blue filters. The results are plotted in Fig. 5. Since the spectral response $P(\lambda)$ of the ITO/P3OT:PCBM/Al is relatively flat in blue and green spectral region (see Fig. 2), the color-matching functions $\bar{g}^S(\lambda)$ and $\bar{b}^S(\lambda)$ are mainly determined by the transmission characteristics of the color filters $F_g(\lambda)$ and $F_b(\lambda)$. The color matching function of the red pixels, however, is determined by both the transmittance of a long wavelength pass filter $F_r(\lambda)$ and the photoresponse of ITO/P3HT:PCBM/Al photodiodes $P(\lambda)$.

4. Color image grabbing

The photodiode array was mounted on a linear translation stage driven by a computer controlled stepping motor. A color image was projected and focused on the surface of the color sensor array. The image was read out by scanning the photodiode array line by line in the longitudinal direction. The 40 dpi resolution was guaranteed by setting the shift step equal to the pixel size of the sensor array. The color information at each position was decomposed into red, green and blue color primaries by placing the red, green and blue filters in sequence in front of the sensor array. The intensity of the image at each color primary was detected by the photodiode with the corresponding color filter. By this process, the color image was collected through three scans and was transformed into three sets of analog photocurrent data matrices.

5. Digitization and image reconstruction

The photocurrent of the P3HT:PCBM color pixels follows a power-law relation with the incident light intensity. A typical data set is shown in Fig. 6. The power index is 0.97, close to unity (i.e., linear photocurrent-intensity dependence). This linear dependence allows the incident light intensity to be represented directly by the photocurrent with negligible deformation. For a digital image with 8-bit dynamic range, the gray levels of the image can be recovered by digitizing the recorded photocurrent data matrices following Eq. (4):

$$\frac{n}{255} = \frac{I}{I_{\max}} = \frac{PC}{PC_{\max}}, \tag{4}$$

where n is the digital color value (an integer between 0 and 255 for 8-bit resolution), I is the light intensity, $I_{\max}$ is the maximum light intensity normalized to the highest gray level 255, and PC and $PC_{\max}$ are the corresponding photocurrents. Eq. (4) can be generalized to image pixels with any power law intensity dependence, i.e. $PC \sim I^{\alpha}$, where α is an arbitrary number. For such a power law, the light intensity can be restored from the recorded photocurrent by the following expression:

$$\frac{I}{I_{\max}} = \frac{PC^{1/\alpha}}{PC_{\max}^{1/\alpha}}. \tag{5}$$

More generally, if the pixel dark current is comparable to the level corresponding to the 1-bit digital gray level (as a result of leakage or other imperfections), this dark current can be corrected during digitalization by the following equation:

$$\frac{n^{r,g,b}}{255} = \frac{I}{I_{\max}} = \frac{(PC^{r,g,b} - DC)^{1/\alpha}}{(PC_{\max}^{r,g,b} - DC)^{1/\alpha}}, \tag{6}$$

where DC is the dark current value.

In our color image reproducing process, the maximum photocurrents measured under the individual r, g, b filters were digitized to 255, and the intensity information contained in the photocurrent data matrices was converted into 8-bit digital data matrices. The dark current of each pixel in the polymer photodiode array was typically three orders of magnitude lower than the maximum photocurrent, which means that no dark current correction was necessary. The final image was recovered by recombination of the red, green and blue mono-color images. Since each color data set was digitized to 8-bit gray levels, a true color resolution (24-bit) was achieved.

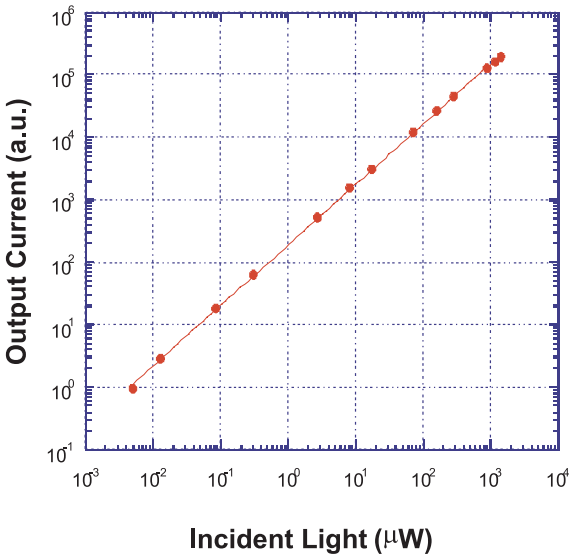

Fig. 6. The light intensity dependence of the photocurrent of the photodiode made with P3HT:PCBM.

Fig. 7 shows a color image recorded with the polymer image sensor and recovered following the procedure describes above. Residual "graininess" in the spatial resolution arises from the 635 μm pixel size. Since image pixels with spatial dimension smaller by an order of magnitude can be fabricated by photolithography, photographic quality true-color images can be achieved with polymer image sensors.

6. Discussion

The color-matching functions of the scanning system can be improved by choosing suitable sensing material, light source or color filters. Improvement by using different color filters has been done in our experiments. Fig. 5 shows the color-matching functions with a set of better filters. In Fig. 7, the color image was scanned by the polymer photodiode array with that set of filters. The image was printed out by an HP DeskJet 1600CM color printer. Since the color printer does not reproduce the color resolution available from the polymer sensor, the original picture and the scanned image printed out by the color printer show no color difference. In addition to the choice of filters, the great variety of the semiconducting polymers offers additional opportunities to match the human visual color-matching functions for accurate color reproduction.

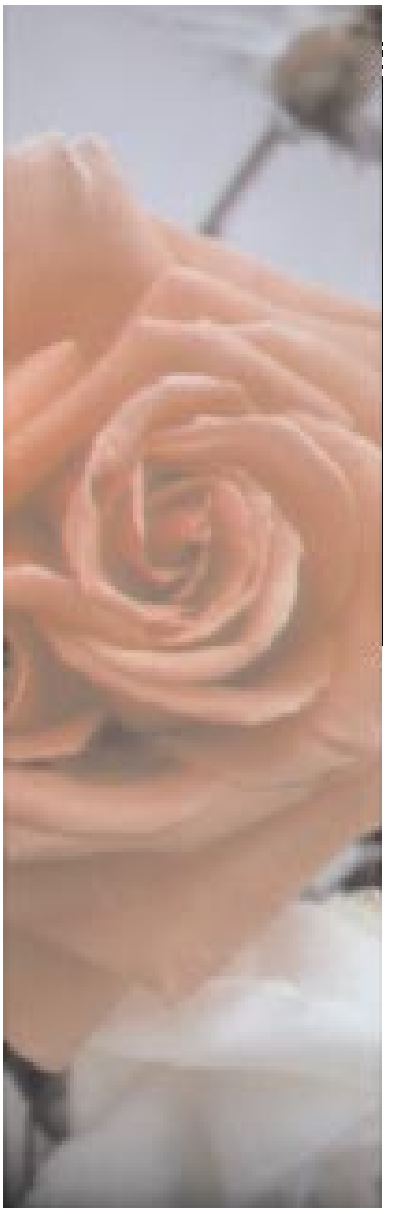

Fig. 7. A scanned image, with true-color resolution, as reconstructed by the computer.

There have been reports in literature that, in some organic photodetectors, the power-law index α of the photocurrent on light intensity derives significantly from unity. The gray level of the input image can be restored accurately by the generalized Eq. (6). We have found from simulations that, for photosensors with α far from unity, this restoration process is a necessary step for correct image reconstruction. The corresponding step in color reproduction of a color display is *gamma* (γ) correction [23]. The restoration step provides a way for any semiconducting polymers with visible spectral response to serve as the sensing material in image sensing applications. In practice, this restoration step can be carried out digitally after recording the image data into a computer. Alternatively, the corrections (dark current subtraction and light intensity restoration) can be carried out by the corresponding circuit unit in the readout circuit prior to digitization. With the correction automatically done during readout, the gray levels of the input image can be read out and digitized directly from the photocurrent following Eq. (4).

The gray levels of the polymer photodiode array are not limited to an 8-bit range. As demonstrated earlier [11–14], the dynamic range of polymer photodiodes is more than six orders of magnitude. This large dynamic range allows 16-bit resolution in each primary color, leading to a combination of 48-bit color resolution. Furthermore, the significant processing advantages of semiconducting polymers allow the photosensors to be fabricated on a curved substrate for detecting light with complicated wavefronts. Thus, polymer image sensor arrays are attractive for high quality imaging applications involving large areas on flexible substrates.

7. Summary

In summary, large area, true-color image sensing with semiconducting polymers has been successfully demonstrated. We have achieved good color primaries by proper selection of color filters and the photosensitive polymer. A generalized equation was developed for digitizing photocurrent with power-law light intensity dependence. By applying this process, any polymer photodiode array with photoresponse that covers the visible spectral range can be used for digital image sensing, including those with non-linear light intensity dependences. The simplicity of the device structure and the processing advantages of conjugated polymers provide unique opportunity for fabricating large area, low cost photodiode arrays, and for using such arrays for large area, high quality image sensing applications.

Acknowledgements

The authors are grateful to Dr. Yong Cao and Dr. Nick Colaneri for stimulating discussions. The work done at UNIAX was supported by the National Science Foundation under Award SBIR Ph II DMI 9801432. The work done at UCSB was supported by the Office of Naval Research (ONR) under N00014-91-J-1235.

References

[1] G. Yu, Metals 80 (1996) 143.
[2] G. Yu, A.J. Heeger, in: M. Scheffler, R. Zimmerman (Eds.), Proceedings of 23rd International Conference on the Physics of Semiconductors, Vol. 1, World Scientific, Singapore, 1996, p. 35.
[3] R. Friend, N. Greenham, in: H. Ehrenreich, F. Spaepen (Eds.), Solid State Physics, Vol. 49, Academic Press, London, 1995, p. 2.
[4] J.H. Burroughes, D.D.C. Bradley, A.R. Brown, R.N. Marks, K. Mackay, R.H. Friend, P.L. Burns, A.B. Holmes, Nature 347 (1990) 539.
[5] D. Braun, A.J. Heeger, Appl. Phys. Lett. 58 (1991) 1982.
[6] I.D. Parker, J. Appl. Phys. 75 (1994) 1656.
[7] I.D. Parker, E. Baggao, P. Bailey, Y. Cao, S. Draeger, H.J. Heeger, J. Kaminski, C. Knudson, J. Long, T. Marx, B. Nilsson, J. Peltola, R. Pflanzer, M. Raffetto, T. Ronnfeldt, B. Weber, G. Yu, C. Zhang, Annual Conference of Society of Information Displays, San Diego, 1998.
[8] I.D. Parker, E. Baggao, P. Bailey, Y. Cao, S. Draeger, A.J. Heeger, J. Kaminski, C. Knudson, J. Long, T. Marx, B. Nilsson, J. Peltola, R. Pflanzer, M. Raffetto, T. Ronnfeldt, B. Weber, C. Zandonatti, Display and Imaging 8 (1999) 15.
[9] I.D. Parker, Y. Cao, C.Y. Yang, J. Appl. Phys. 85 (1999) 2441.
[10] Y. Cao, I.D. Parker, G. Yu, C. Zhang, A.J. Heeger, Nature 397 (1999) 414.
[11] G. Yu, Y. Gao, J.C. Hummelen, F. Wudl, A.J. Heeger, Science 270 (1995) 1789.

[12] G. Yu, A.J. Heeger, J. Appl. Phys. 78 (1995) 4510.
[13] G. Yu, C. Zhang, A.J. Heeger, Appl. Phys. Lett. 64 (1994) 1450.
[14] G. Yu, K. Pakbaz, C. Zhang, A.J. Heeger, J. Electron Mater. 23 (1994) 925.
[15] G. Yu, J. Wang J, J. McElvain, A.J. Heeger, Adv. Mater. 17 (1998) 1431.
[16] N.S. Sariciftci, L. Smilowitz, A.J. Heeger, F. Wudl, Science 258 (1992) 1474.
[17] C.H. Lee, G. Yu, D. Moses, K. Pakbaz, C. Zhang, N.S. Sariciftci, A.J. Heeger, F. Wudl, Phys. Rev. B 48 (1993) 15425.
[18] G. Yu, G. Srdanov, H. Wang, Proceedings of SPIE, Vol. 3939, 2000.
[19] R.P. Feynman, R.B. Leighton, M. Sands, The Feynman Lectures on Physics, Vol. 1, Addison-Wesley, Redwood City, 1989.
[20] R.W.G. Hunt, Measuring Color, Wiley, New York, 1987.
[21] D.B. Judd, G. Wyszecki, Color in Business, Science and Industry, Wiley, New York, 1975.
[22] P.C. Hung, Camera and Input Scanner Systems, SPIE, Vol. 1448, 1991, p. 164.
[23] C.A. Poynton, A Technical Introduction to Digital Video, Wiley, New York, 1996.